論 文

Comparison of Four Different Latent Heat Models During the Melting Process

Jong-Hyun Kim*, In-Cheol Lim**, Sung-Sik Kim***

용융시 수반되는 4가지 다른 잠열 모델의 비교 연구

김 종 현*, 임 인 철**, 김 성 식***

초 록

상변환시 수반되는 경계면에서의 잠열의 방출(또는 흡수)의 정확한 해석은 용접, 주조, 결정 생성, 일기 예보 등의 응용에 필수적인 것이다. 특히 주조의 경우 캐스팅 온도와 고체 용적분율의 관계를 앎으로서 잠열 방출의 해석이 가능하다.

본 연구는 상변환시 수반되는 잠열의 방출 형태를 4개의 다른 모델을 사용하여 비정상 온도분포, 용융형태, 자연대류가 미치는 영향을 수치적으로 구하였다. 2개의 서로 다른 물성치를 가진 합금을 선택하였는데 하나는 넓은 mushy 영역을 가진 알루미늄 합금이고 다른 하나는 좁은 mushy 영역을 가진 철금속계 합금이다. 알루미늄 합금의 경우 온도 분포와 시간에 따른 온도의 변화가 모델에 따라 상당한 차이가 있는 반면 철금속계 합금의 경우 상이한 모델일지라도 거의 차이가 없음을 알 수 있었다.

결론으로 용융시 정확한 온도 분포와 상변화 형태를 예측하기 위해서는, 알루미늄 합금(넓은 mushy 영역)의 경우 적절한 잠열 방출 모델의 채택이 필요 불가급한 것으로 사료된다.

1. Introduction

Problems which involve a phase-change are of great physical significance in engineering applications such as casting, welding, crystal growth, freezing of food, weather prediction and so forth. A typical illustration of the phase change phenomena is the melting and solidification process. This is a complex process that involves a coupling between heat/mass transfer and fluid flow, and in most cases which does not yield an exact analytical solution. The experiment of measuring the temperature change and of locating the boundaries defining three regions is extremely difficult to perform. Hence numerical analysis is essential tool to predict the behaviour of phase change process. Numerical modeling of the phase-change processes is inherently difficult due to the requirement that the momentum equation, energy equation, and continuity equation, together with interface boundary conditions must be solved simultaneously. Moreover,

*Research Engineer(Ph.D.), School of Mechanical Eng.

**Graduate Student, School of Eng., Science and Mechanics, G.I.T., Atlanta Ga. 30332, U.S.A.(미국 조지아 공과대)

***Assistant Professor (Ph.D.), Department of Inorganic Materials Eng., Hong Ik University.(홍익대 무기재료공학과)

due to the transient nature of this process, moving interface locations should be considered in the model. Therefore, many assumptions and constraints are required to obtain the solution for transient temperatures in phase-change processes.

In this paper, the transient phase-change process together with the specific heat method is examined. The specific heat method [1-9] in conjunction with latent heat release (or absorption) models is used to solve the coupled momentum and energy equations. The latent heat release (or absorption) models considered include the linear [1-11], quadratic [10], lever rule [10-11] and Scheil's equation [10-11]. Generally, the linear model has been widely used because of its simplicity.

In this study, two distinct alloys-one with a wide mushy zone and the other with a narrow mushy zone-have been chosen to investigate the temperature histories, the melting pattern and the effect of natrual convection for the four proposed models. A comparison will be made to examine the differences for these proposed algorithms under the same condition.

2. Governing Equations

From mass conservation, the continuity equation can be expressed as

$$\frac{\partial \rho}{\partial t} + (\rho u_j)_{,j} = 0 \qquad (1)$$

Application of the principle of conservation of linear momentum to the fluid elements leads to

$$\rho\left[\frac{\partial u_i}{\partial t} + u_j u_{i,j}\right] = \sigma_{ij,j} + \rho f_i \qquad (2)$$

For the fluid, the stress tensor can be written as :

$$\sigma_{ij} = -p\delta_{ij} + \tau_{ij} \qquad (3)$$

The energy equation for phase change problems based on the enthalpy formulation can be rewritten in a cartesian coordinate as :

$$\rho c_p\left[\frac{\partial T}{\partial t} + u_i T_{,i}\right] = (kT_{,j})_{,j} + q_s \qquad (4)$$

In order to solve the phase change problem in the mushy zone, the source term, q_s, in equation (4) is defined as a time dependent latent heat release, or,

$$q_s = \frac{\partial}{\partial t}\rho L(1-f_s) \qquad (5)$$

Note that the latent heat release at the interface is a linear function of the solid fraction, f_s and it is assumend that the density variation is negligible in each phase. To understand the temperature behaviors during the phase change process, four different relationships between the solid fraction and the casting temperatures are considered. The first algorithm is a linear model, in which the latent heat release changes linearly between the solidus and liquidus temperatures. This relationship is represented as :

$$f_s = \frac{T_{liq} - T}{T_{liq} - T_{sol}} \qquad T_{sol} \le T \le T_{liq} \qquad (6)$$

where T_{sol} and T_{liq} represent the solidus and liquidus temperatures respectively.

The second algorithm is a quadratic model where the latent heat release is changing quadratically at the interfaces. This numerical formulation is given as :

$$f_s = \left[\frac{T_{liq} - T}{T_{liq} - T_{sol}}\right]^2 \qquad T_{sol} \le T \le T_{liq} \qquad (7)$$

The third model of the latent heat release is called the lever rule, in which the complete equilibrium between the solid and liquid phases is maintained throughout the process. The lever rule yields,

$$f_s = \frac{1}{1-P}\left[\frac{T - T_{liq}}{T - T_m}\right] \quad T_{sol} \le T \le T_{liq} \qquad (8.1)$$

and

$$P = \frac{T_m - T_{liq}}{T_m - T_{sol}} \qquad (8.2)$$

where P is the equilibrium partition ratio and T_m is the fusion temperature of the pure ma-

terial.

The fourth mode of latent heat release, assuming infinite diffusion in the liquid phase and no diffusion in the solid phase, yields the following Scheil's equation :

$$f_s = 1 - \left[\frac{T - T_m}{T_{liq} - T_m}\right]^{\frac{1}{p-1}} \qquad T_2 \le T \le T_{liq} \quad (9)$$
$$= 1 \qquad T = T_e$$

Here, T_e is the eutectic temperature of the material. It is also worth noting that the amount of latent heat release for these four different modes is the same although the rates at which the latent heat release (absorption) occurs is different.

The governing equations (1)－(3) are nondimensionalized to measure the relative importance of various terms and to identify the dominant physical parameters. The following dimensionless quantities are introduced to simplify the governing equations :

$$U = \frac{\alpha}{l}\sqrt{RaPr}\ , \quad (10.1)$$

$$u^* = \frac{u}{U} \quad T^* = \frac{T - T_1}{T_2 - T_1} \quad x^* = \frac{x}{l}\ ,$$

$$p^* = \frac{pl}{\mu U} \qquad t^* = \frac{\nu t}{l^2}\ . \quad (10.2)$$

By substituting equations (10.1)－(10.2) into equations (1)－(3), the nondimensional governing equations can be expressed as follows :

$$\nabla u^* = 0\ , \quad (11)$$

$$\frac{\partial u^*}{\partial t^*} + \sqrt{\frac{Ra}{Pr}}u^* \cdot \nabla u^* = -\nabla p^* + \nabla^2 u^* + \frac{l^2}{\nu U} f_v \quad (12)$$

$$\frac{1}{Pr}\frac{\partial T^*}{\partial t^*} + \sqrt{RaPr}\,u^* \cdot \nabla T^* \quad (13)$$
$$= \nabla^2 T^* + \frac{q_s l^2 (T_2 - T_1)}{k}$$

where the Rayleigh and Prandtl numbers are defined as :

$$Ra = \frac{\rho\beta g(T_2 - T_1)l^3}{\mu\alpha} \quad (14)$$

and

$$Pr = \frac{\nu}{\alpha} = \frac{\mu C_p}{k} \quad (15)$$

Using the above dimensionless quantities and nondimensional equations, the physical properties of the equation are replaced by the following quantities :

$$\rho = \sqrt{\frac{Ra}{Pr}}$$
$$c_p = Pr$$
$$\mu = 1.0 \quad (16)$$
$$g = 1.0$$
$$k = 1.0$$

2.1 Solution Procedures and Problem Description

To make a quantitative assessment of the latent heat release during the phase change process, two different mushy zones are chosen to be used with the four different latent heat release models. One has a wide mushy zone and the other has a narrow mushy zone.

The latent heat release models, equations (6)－(9), are substituted into the source term in the energy equation to account for the phase change. The enthalpy formulation (or specific heat method) requires no explicit conditions on the heat flow at the interface. Thus, it is possible to use a fixed grid scheme, which is beneficial since it simplifies the numerical modeling requirements.

The numerical technique used in this study is based upon the finite element method, using the Galerkin formulation. A detailed description of the Galerkin method can be found in the References [12, 13]. As is discussed in these references, an overrelaxation factor is used for the wide mushy zone to increase the time integration parameter while an under-relaxation factor is used for the narrow mushy zone to maintain the numerical

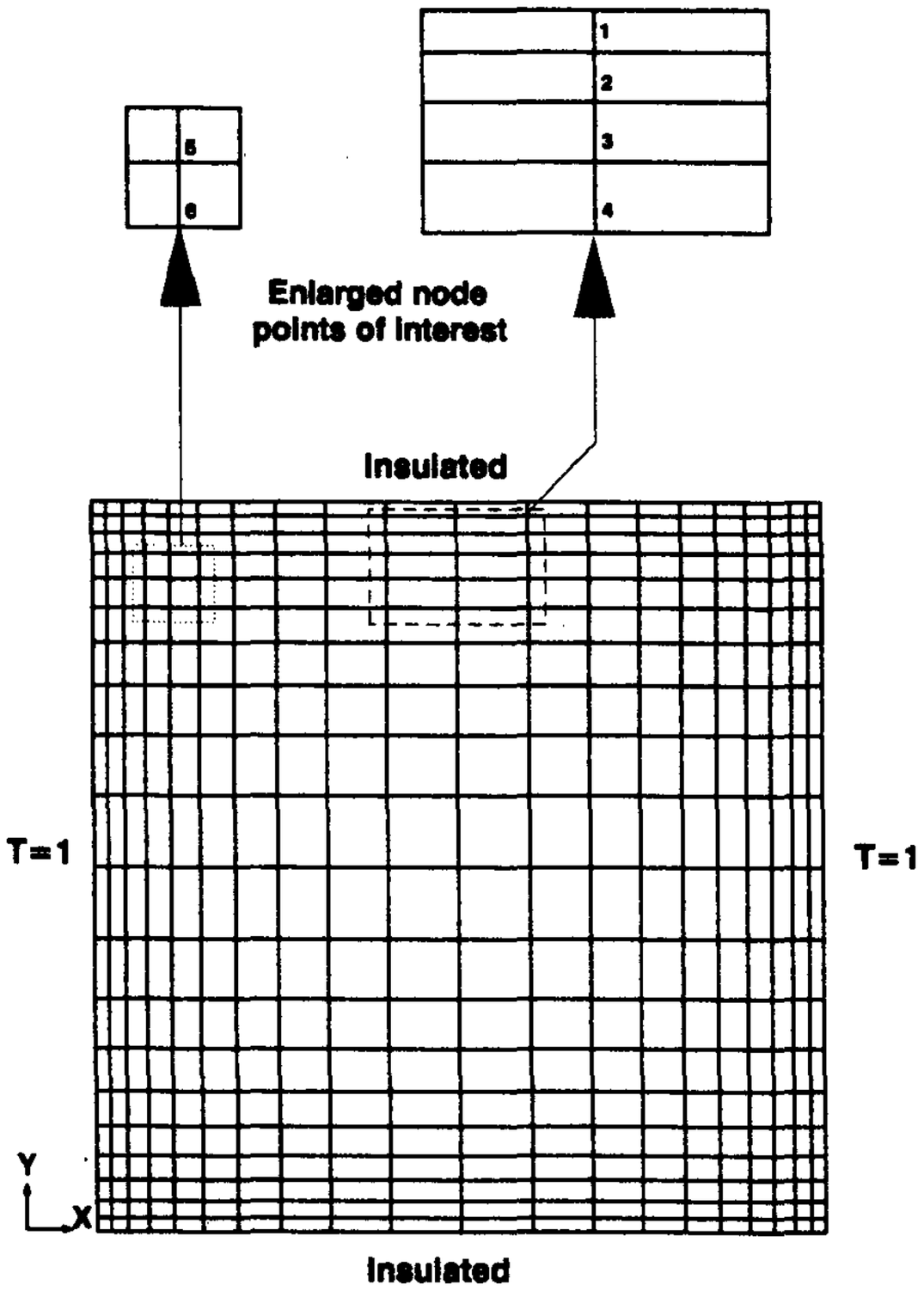

Figure 1. Numerical domain, boundary conditions and selected points to obtain the temperature histories.

convergence. Generally, the viscosity of the solid metal is over 20 orders of magnitude higher than that of the liquid metal [11]. Hence large values of viscosity are assigned in the solid phase when its temperature falls below the melting temperature to ensure that the velocity is zero in the solid phase.

The numerical domain and its boundary conditions are shown in Figure 1. A fine grid mesh was chosen near the walls because of the high temperature gradient resulting from natural convection. A coarse grid mesh was chosen in the middle of the cavity. Definitions for the physical input paramenters is shown in equation (16) and the resulting input paramenters for the two different mushy zones are listed in Table 1.

Table 1. Input data for a wide mushy zone. (nondimensional values)

Density	316.2
Specific heat (liquid phase)	0.08
Specific heat (solid phase)	0.1
Viscosity (liquid phase)	1.0
Viscosity (solid phase)	10^{20}
Gravity	1.0
Thermal conductivity	1.0
Temperature of liquidus	0.9
Temperature of solidus	0.7
Fusion temperature	0.93
Eutectic temperature	0.76
Rayleigh number	10000
Prandtl number	0.1
Latent heat	5.0

Table 2. Input data for a narrow mushy zone. (nondimensional values)

Density	316.2
Specific heat (liquid phase)	0.08
Specific heat (solid phase)	0.1
Viscosity (liquid phase)	1.0
Viscosity (solid phase)	10^{20}
Gravity	1.0
Thermal conductivity	1.0
Temperature of liquidus	0.75
Temperature of solidus	0.7
Fusion temperature	0.76
Eutectic temperature	0.71
Rayleigh number	10000
Prandtl number	0.1
Latent heat	5.0

3. Results and Discussions

Two different mushy zones were selected in this paper. One has a wide mushy zone, ($T^*_{liq} - T^*_{sol} = 0.2$), and the other has a narrow mushy zone, ($T^*_{liq} - T^*_{sol} = 0.05$). Initially, the whole domain has a value of $T^* = 0$. For two different mushy zones, four different latent heat models are used to calculate the

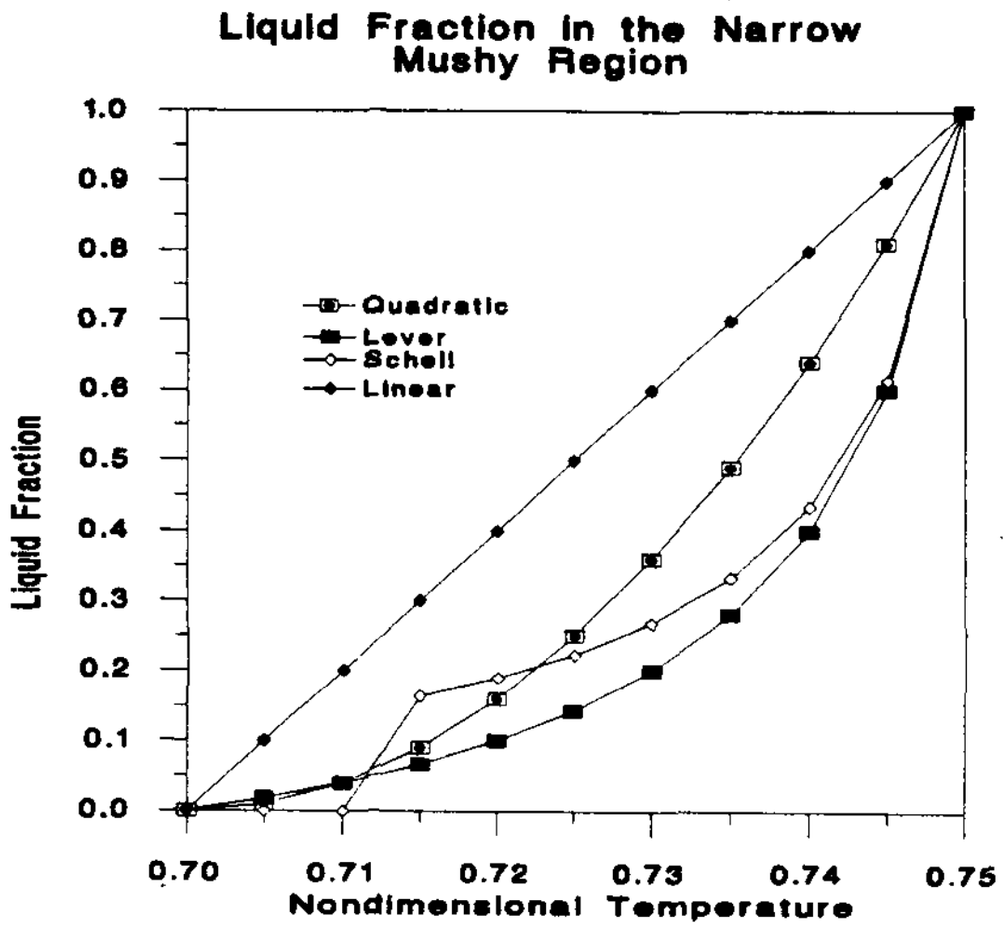

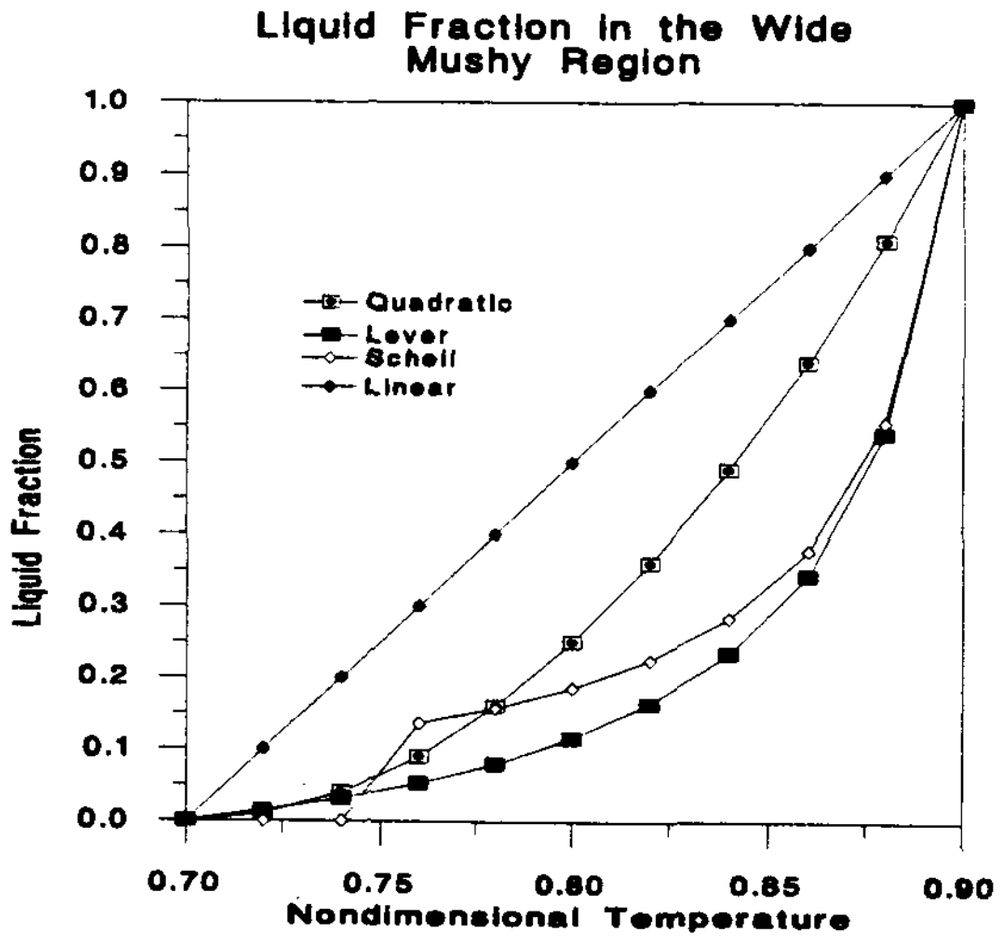

Figure 2. Liquid fraction versus nondimensional temperature.

temperature history, the melting pattern and the effect of natural convection during the phase change process. The relationships between the liquid fraction and phase change temperatures for the four different models are shown in Figure 2. The difference in the rate of latent heat absorption in the mushy zone for each model is well exhibited in this figure. At the early stage of the melting process, a maximum of heat is absorbed in the linear model, and minimum amount of heat is

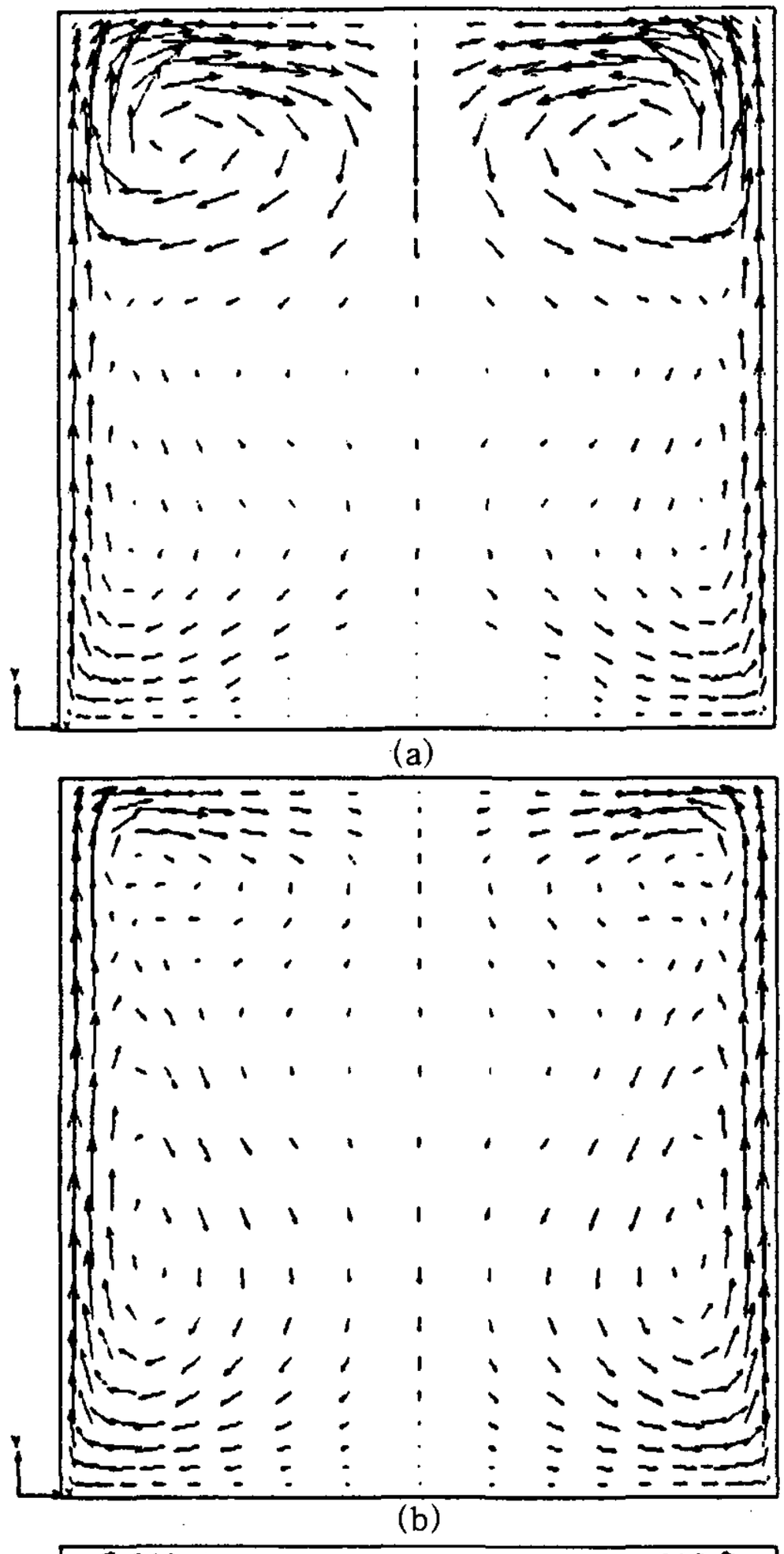

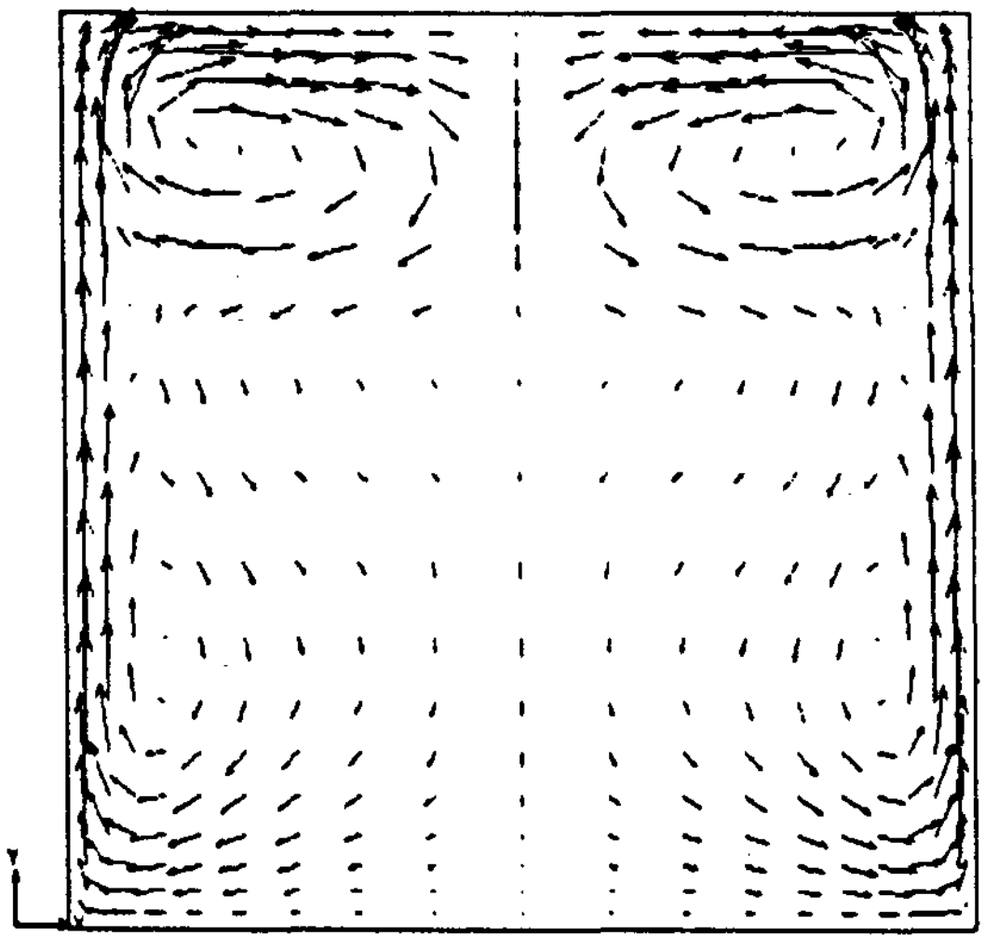

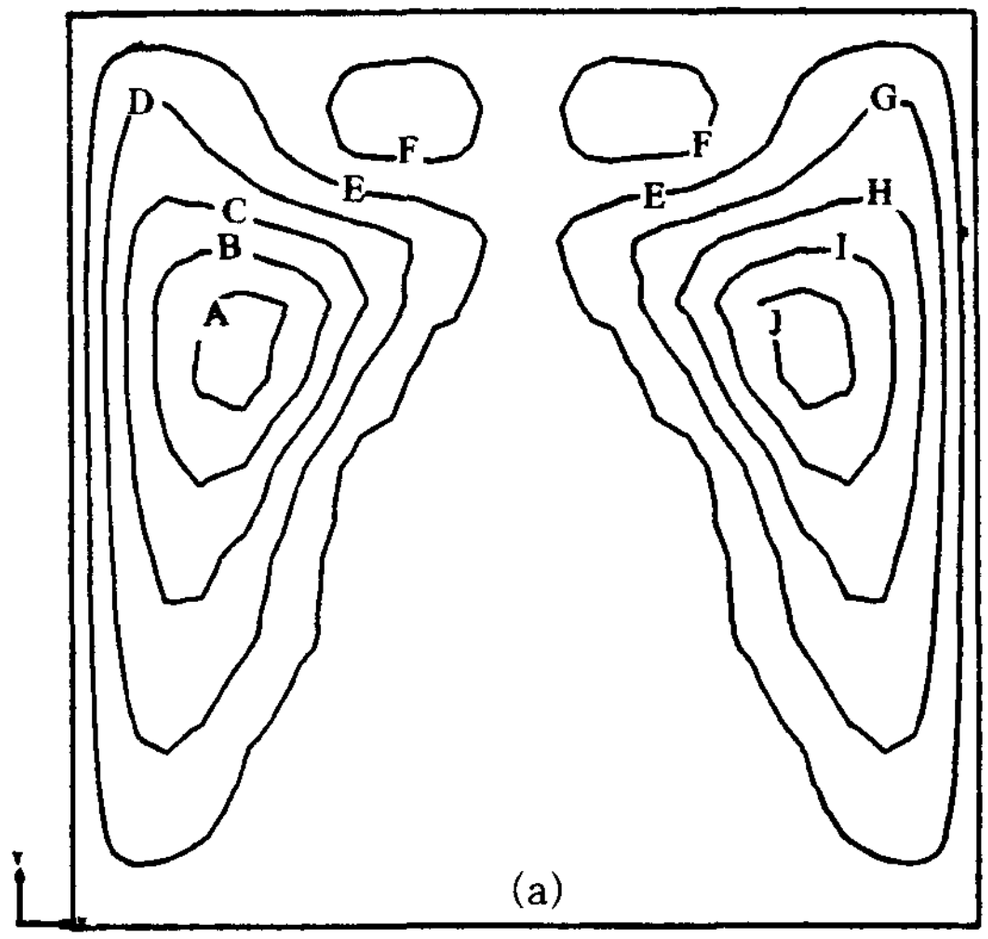

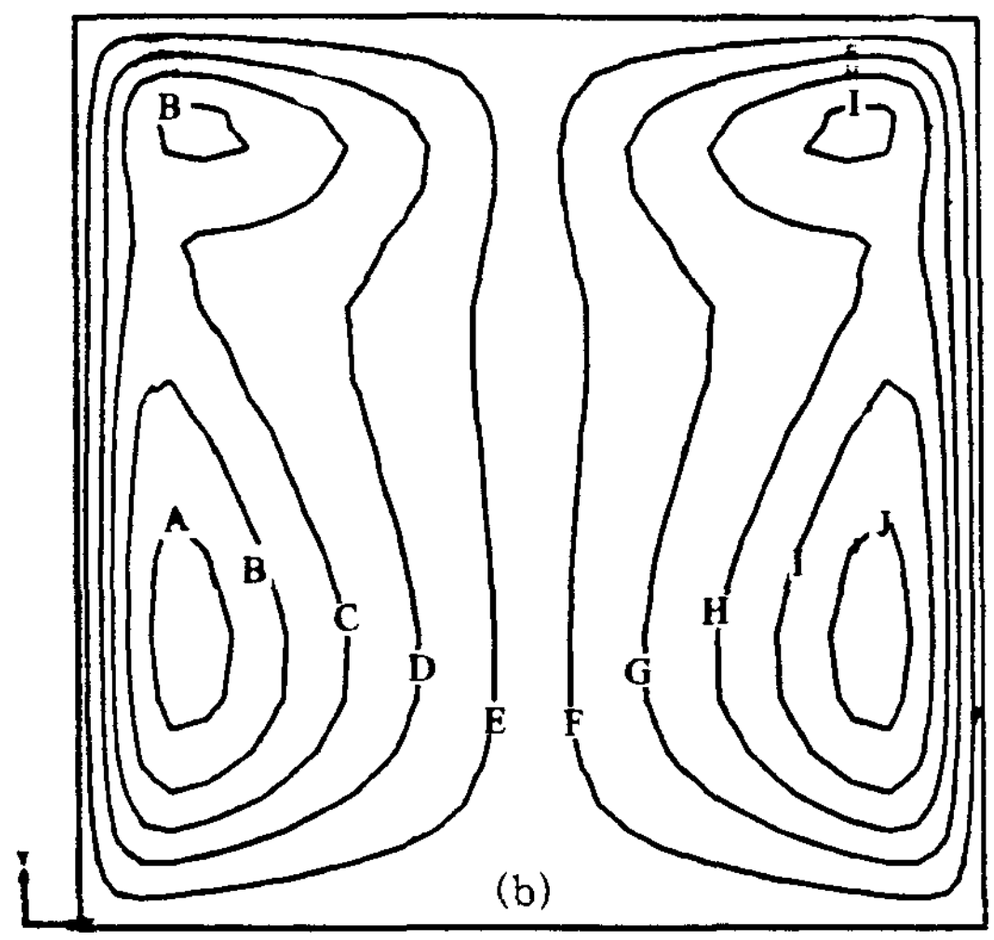

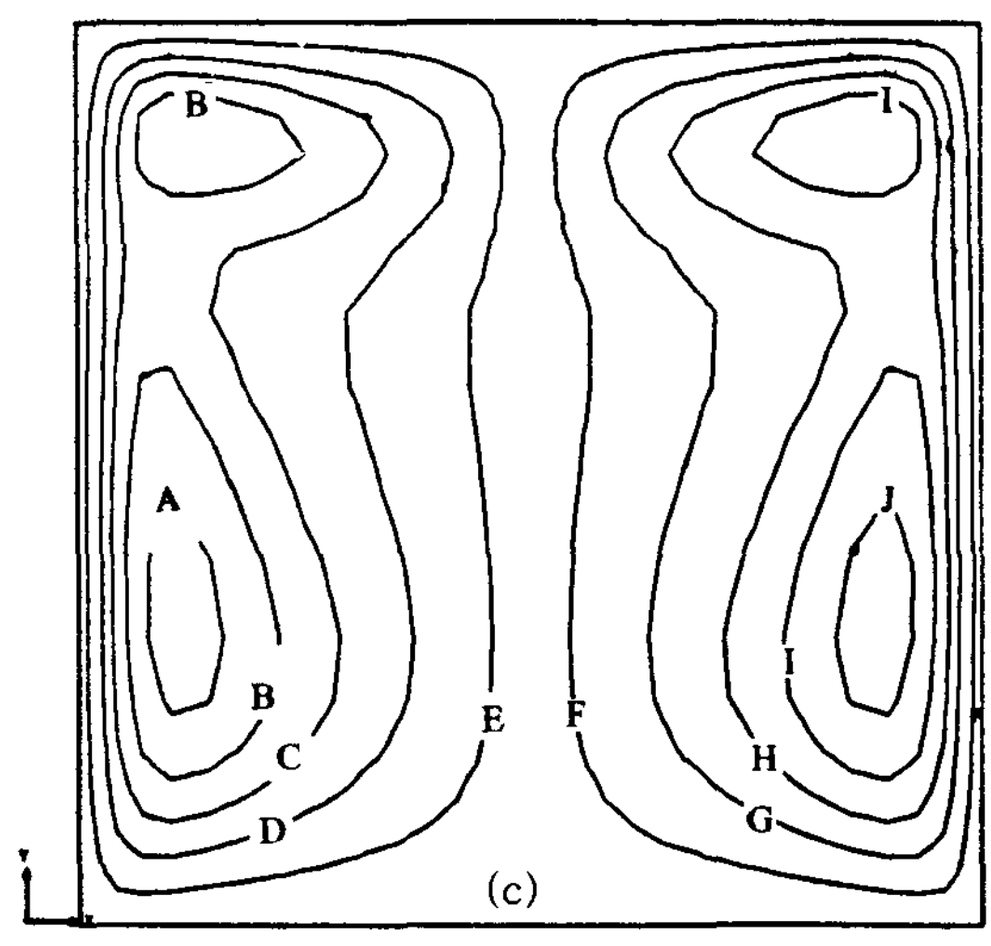

Figure 3. Velocity vectors for a wide mushy region at time, $t^*=179$. (a) Linear model, (b) Quadratic model, (c) Lever rule, and (d) Scheil's equation.

absorbed in the Scheil's and the lever rule. However, in the early period of the solidification process, a minimum of heat is released in the linear model, and maximum amount of heat is released in the Scheil's and lever rule.

Figure 3 depicts the velocity profiles of the four different models at the nondimensional time, $t^*=179$. In all cases, strong velocity motions are found near the side walls due to the high temperature at the walls. Circular motions in the top zone are apparent because of the natural convection. In the linear model, the velocity motion is not found in the bottom of cavity because the melting has not occurred at time, $t^*=179$. The streamline for each case is shown in Figure 4. Depending on the rate at which heat is absorbed, it is obvious that the fluid motions are different for each model.

Figure 5 represents the isothermal lines at the time, $t^*=179$. Similar temperature distributions are found in the Scheil's, the

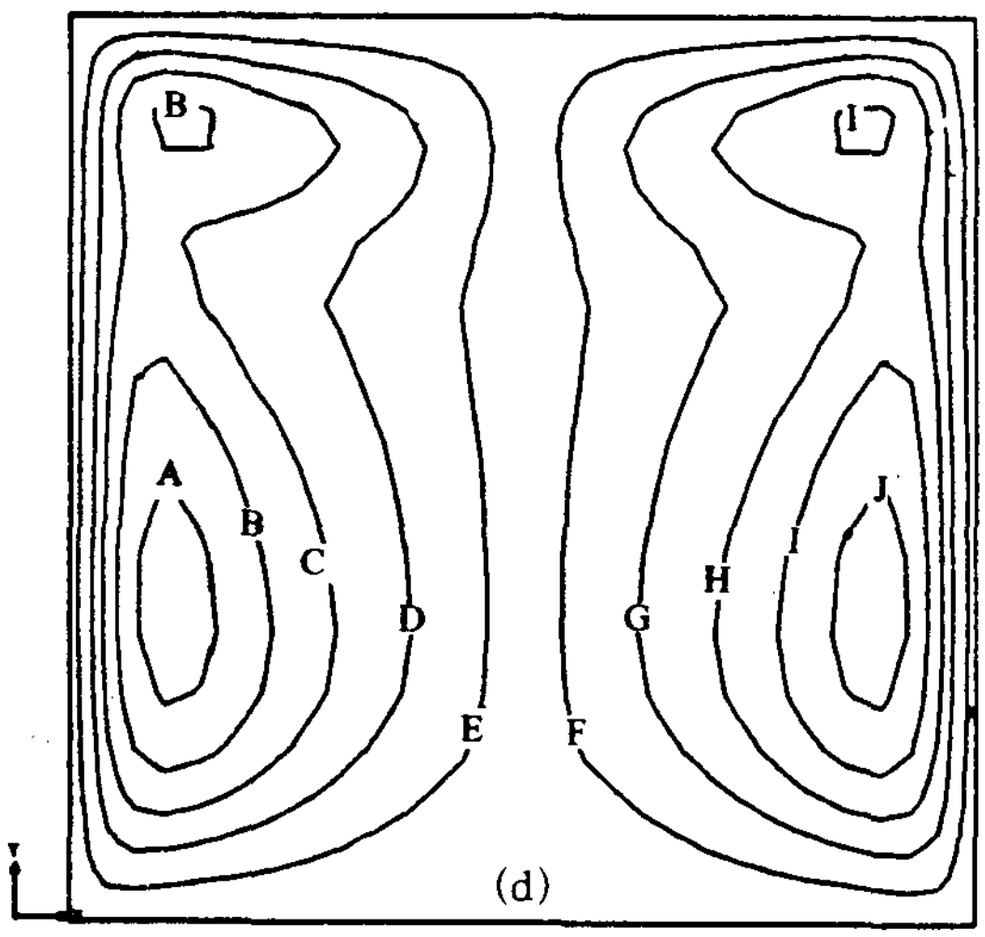

Figure 4. Streamlines for a wide mushy region at time, $t^*=179$. (a) Linear model, (b) Quadratic model, (c) Lever rule, and (d) Scheil's equation.

lever and the quadratic model, while the linear model shows a different temperature profile due to the unmelted zone in the middle of cavity. Figure 6 shows the temperature history of the different latent heat models at selected points (node No. 1－4) in the wide mushy zone. Significant temperature differences are observed in the mushy zone where the latent heat absorption has occurred. The maximum discrepancies in temperature profiles are found between the linear model and the Scheil's rule or the lever rule. The linear model requires the most time to obtain the complete melting compared to the other models ; whereas the least time would be required in solidification.

To examine the mushy zone during the melting process, time, $t^*=140$, is also chosen. The isothermal lines in each case are shown in Figure 7. *A*, *B* and *C* represent the nondimensional temperatures, 0.7, 0.8 and 0.9, respectively. The mushy zone is located between *a* and *c*. As it is shown in Figure 7 (a), linear model has a larger solid region, while the other three models have similar solid regions. Figure 7 distinct the difference of the melting behaviors in each model.

The temperature history in the narrow mushy zone (node No. 5－6) is shown in Figure 8 for the four different latent heat models. The temperature curves in the mushy zone for the four different cases are nearly coincident each other, since the latent heat absorption occurs between a narrow temperature band.

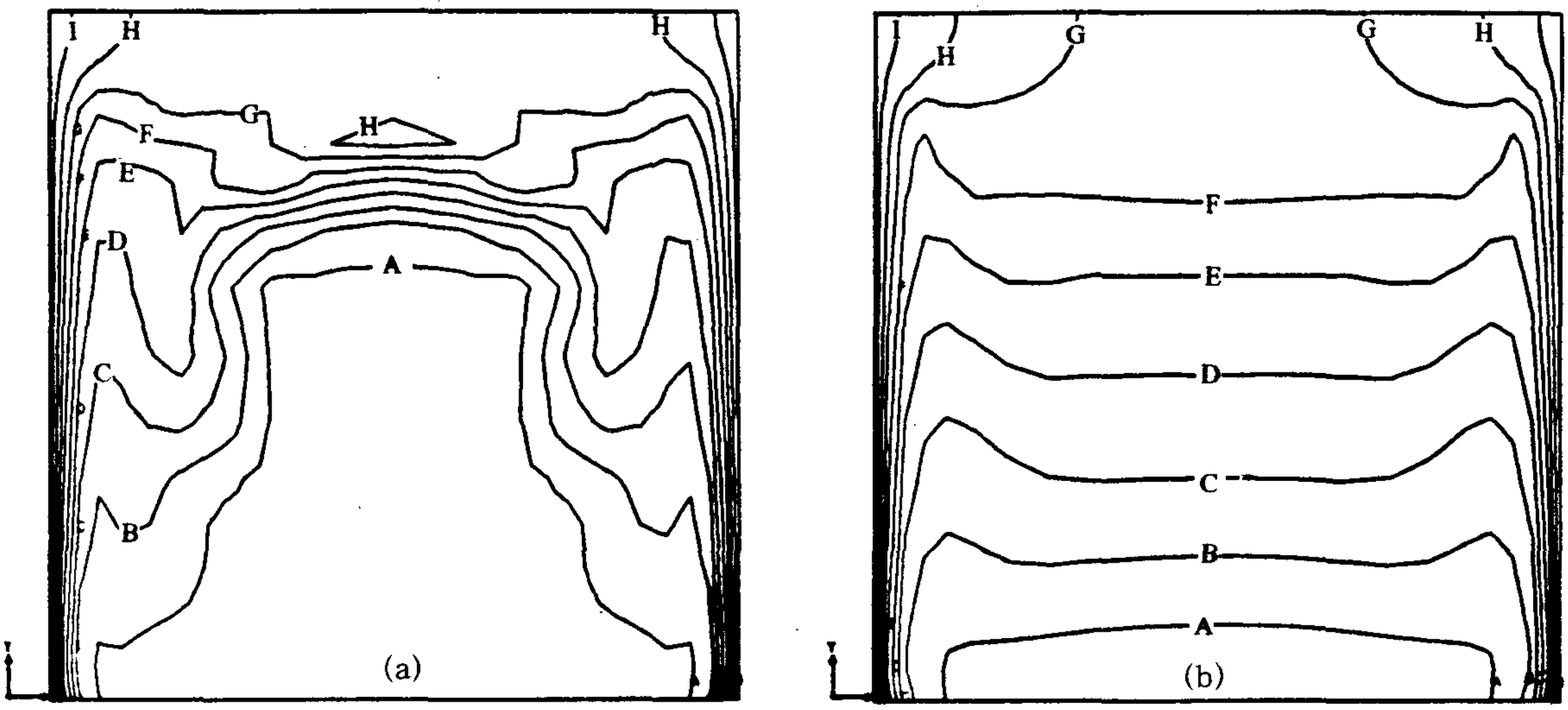

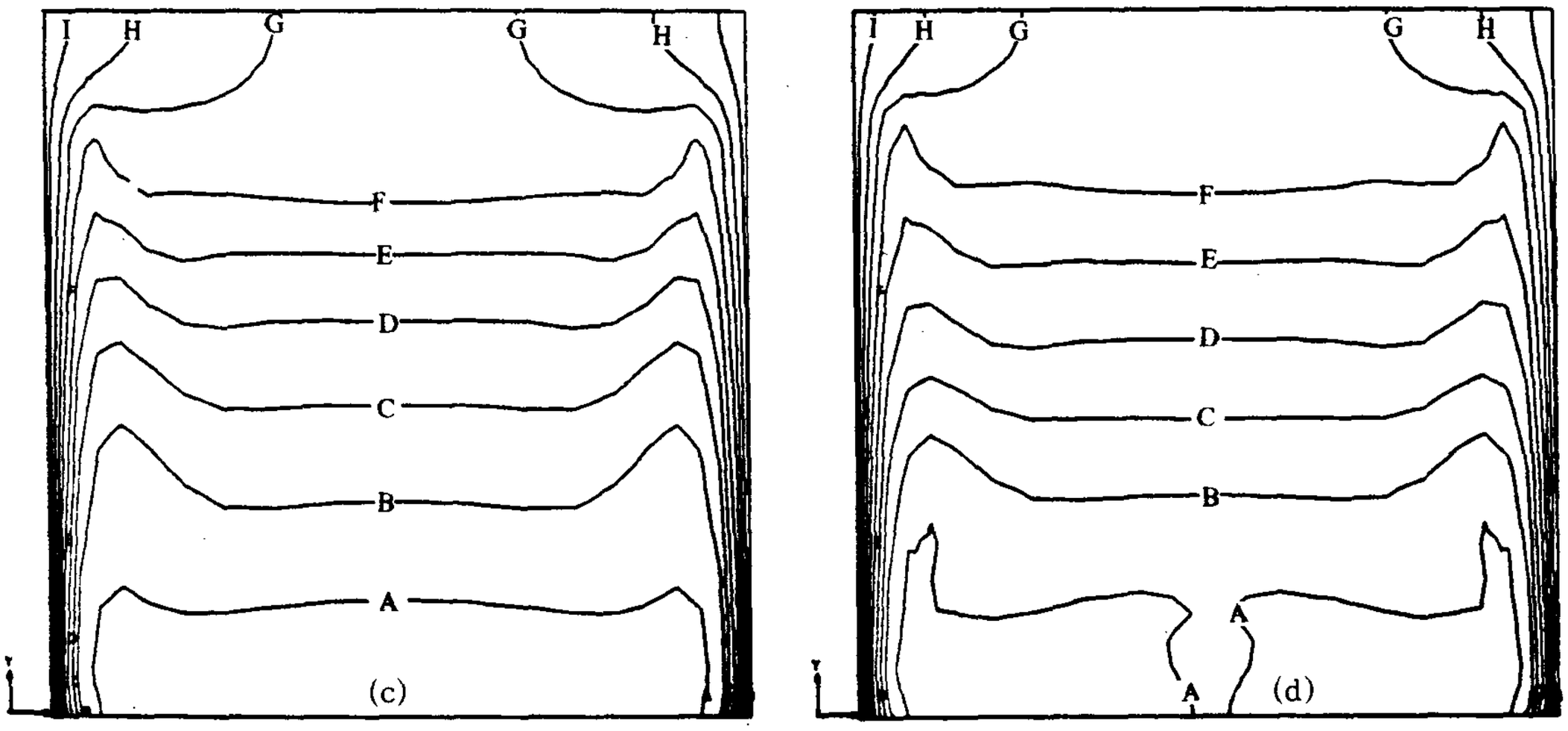

Figure 5. Isotherms for a wide mushy region at time, $t^* = 179$. (a) Linear model, (b) Quadratic model, (c) Lever rule, and (d) Scheil's equation.

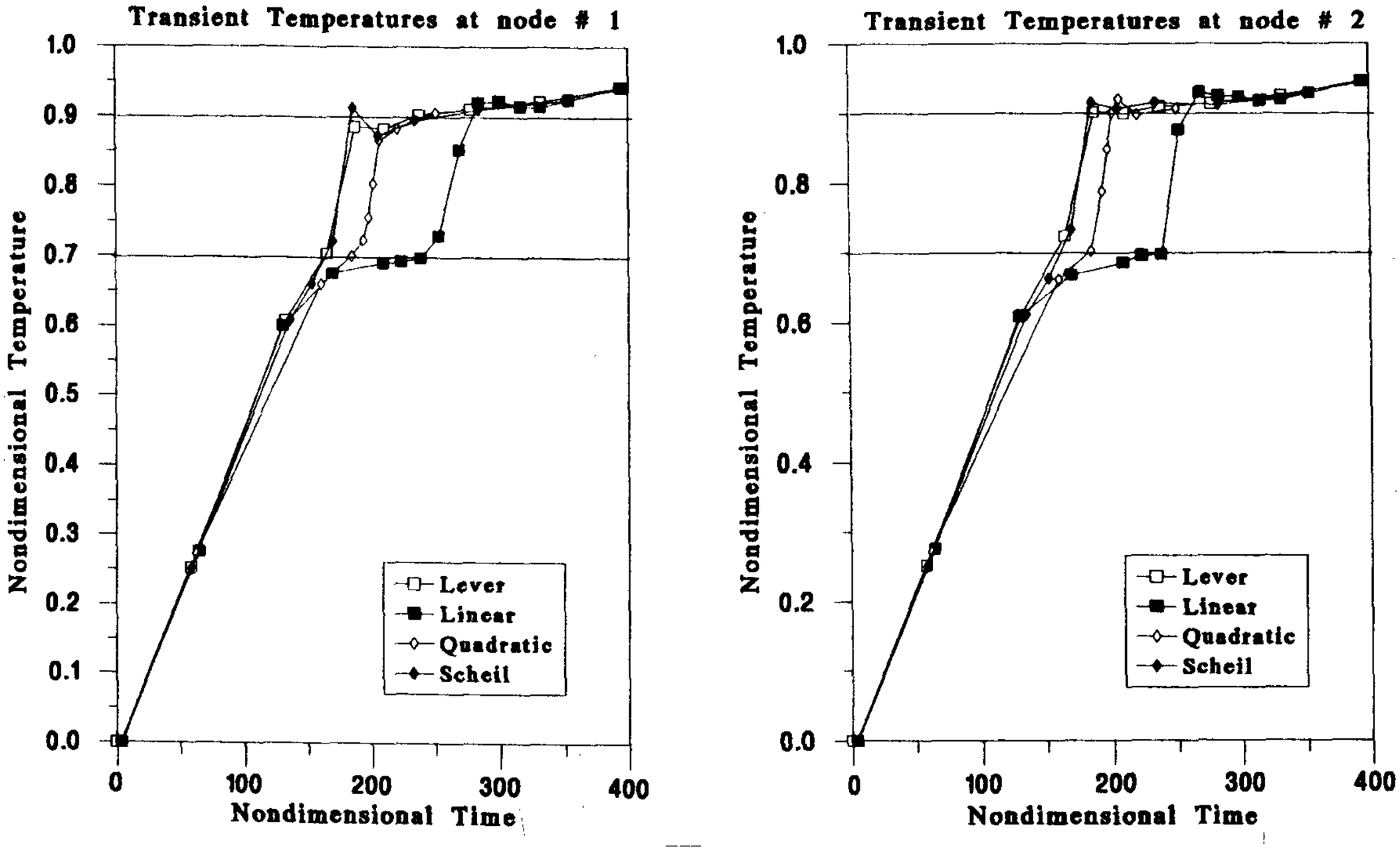

Figure 6. (a). Temperature histories for a wide mushy region at selected node points 1 and 2.

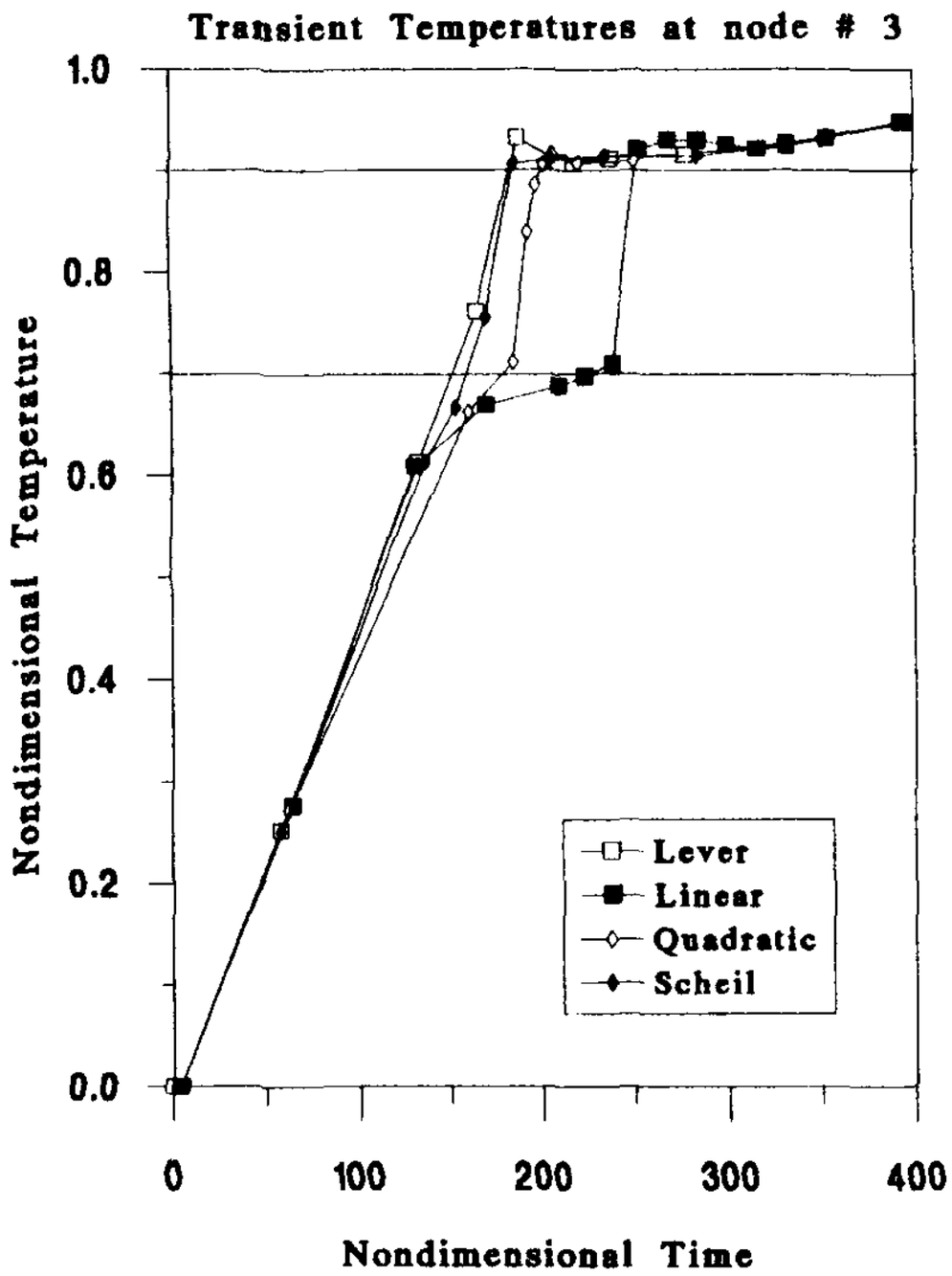

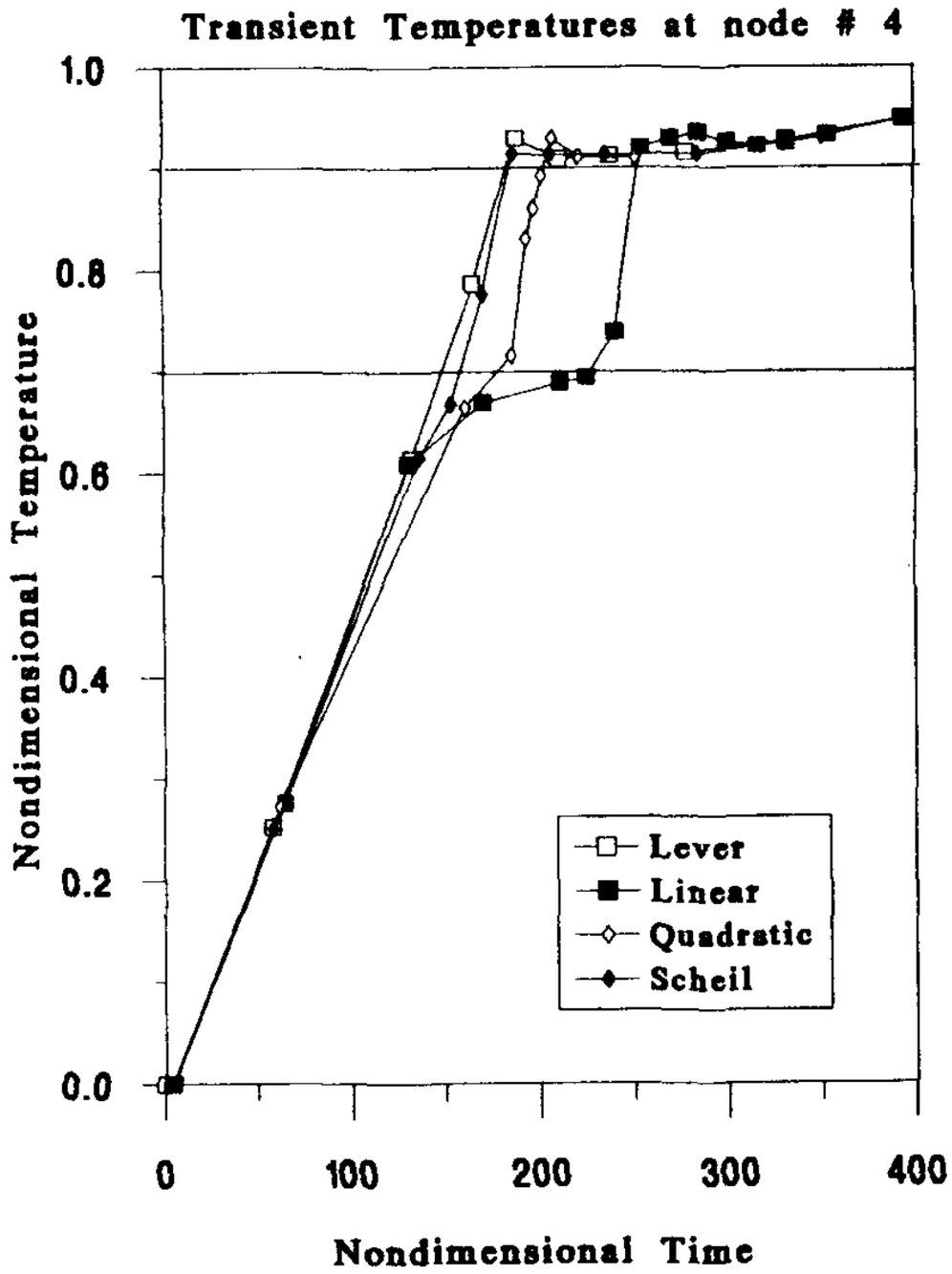

Figure 6. (b). Temperature histories for a wide mushy region at selected node points 3 and 4.

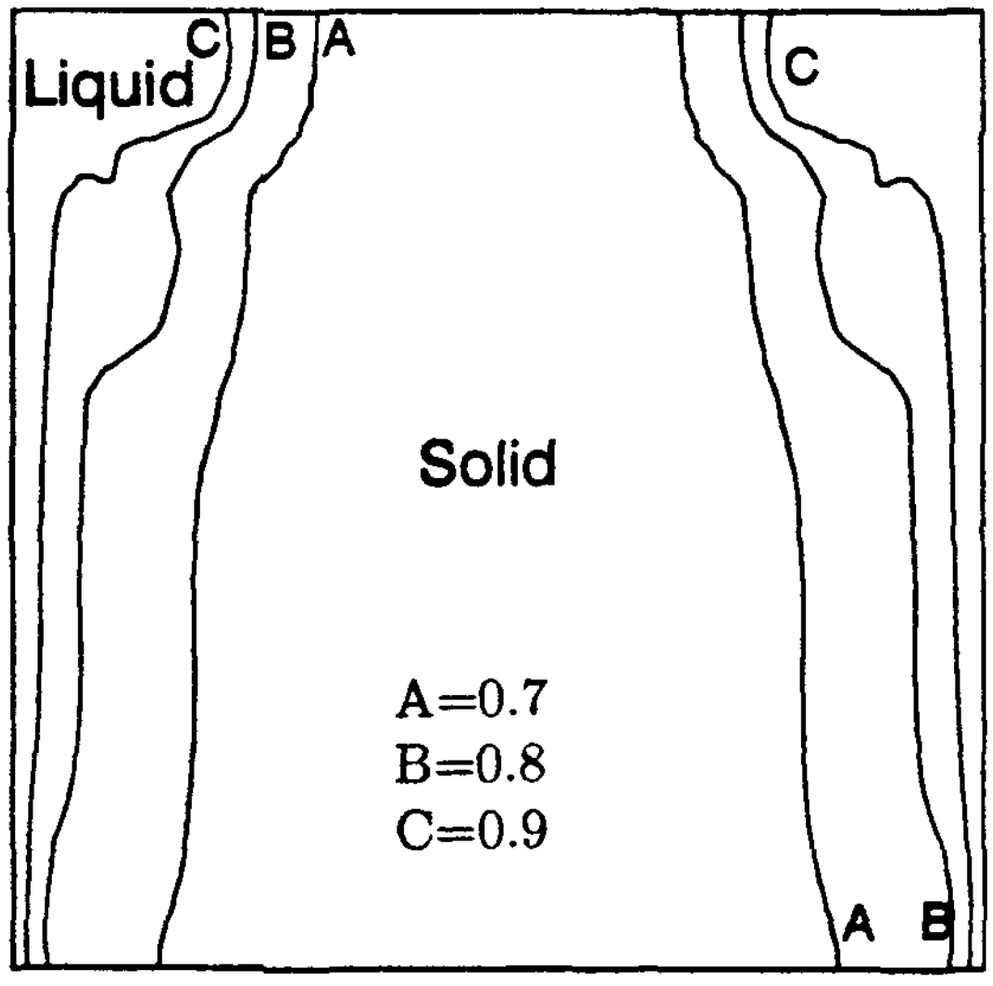

(a)

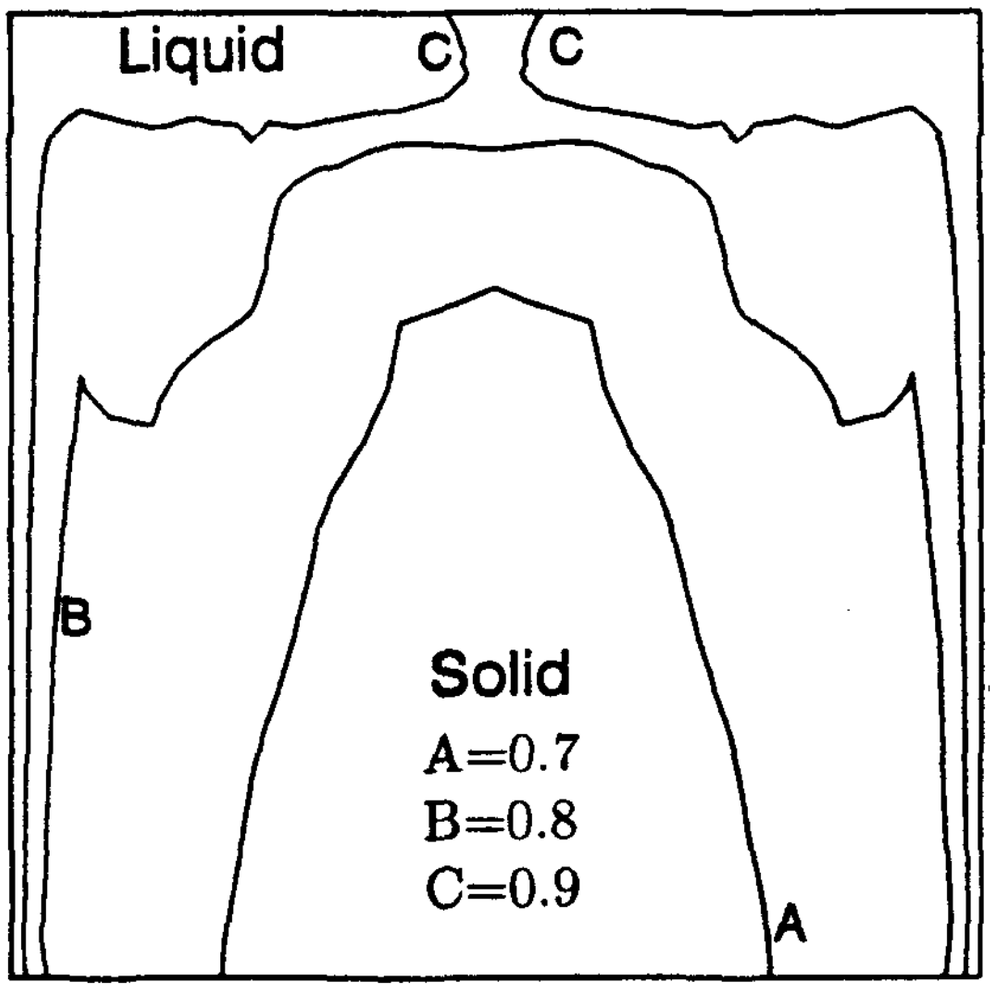

(b)

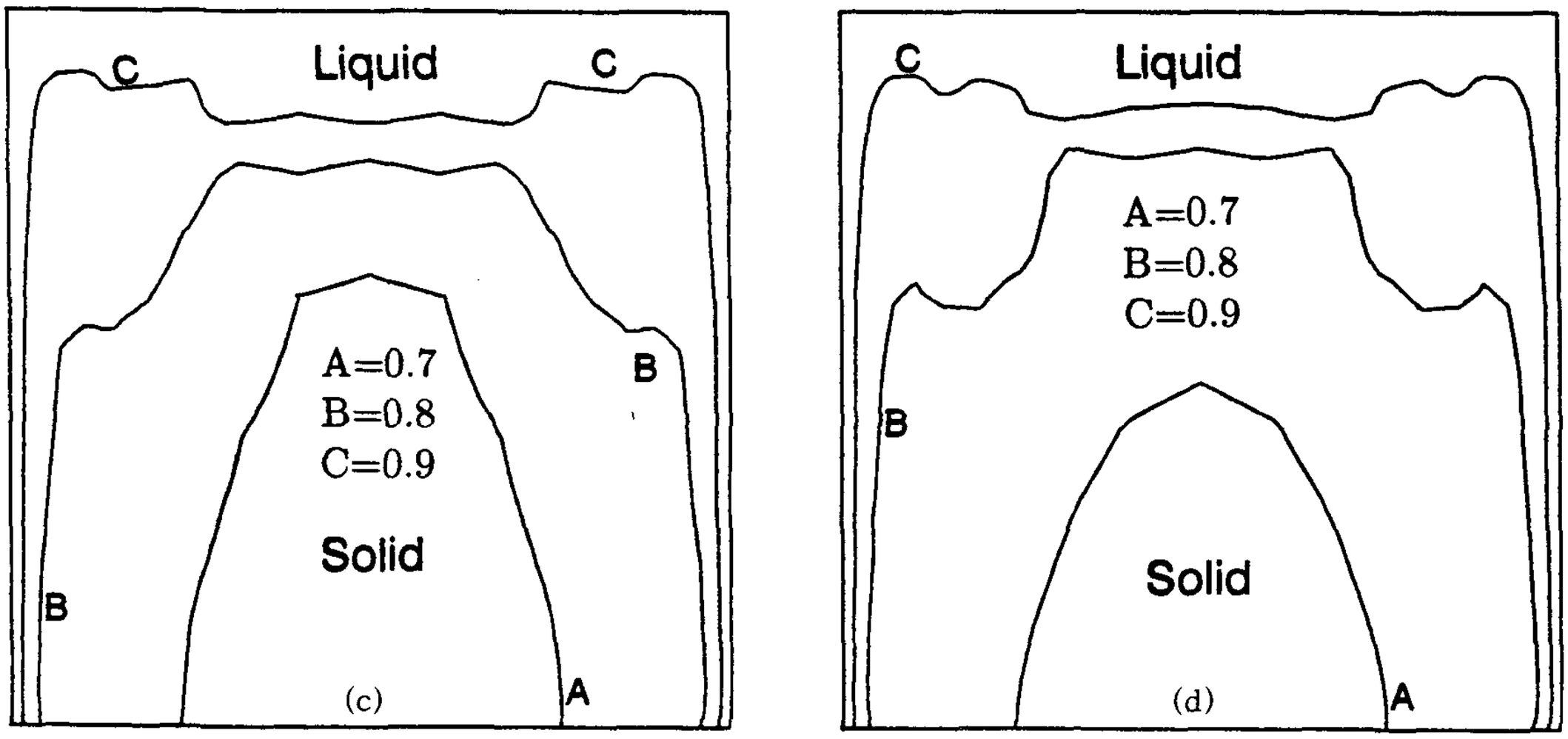

Figure 7. Isotherms for a wide mushy region at time, $t^* = 140$. (a) Linear model, (b) Quadratic model, (c) Lever rule, and (d) Scheil's equation.

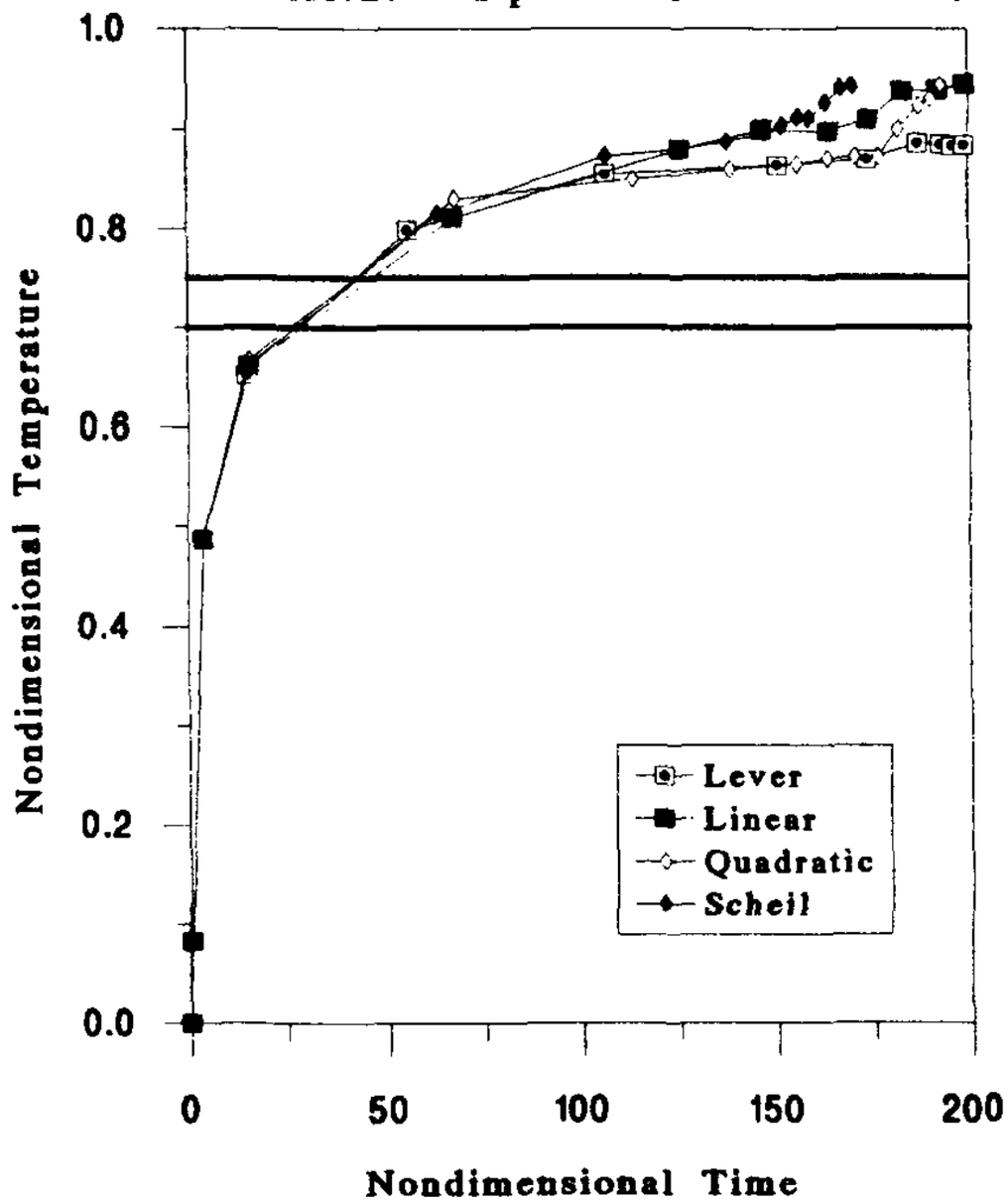

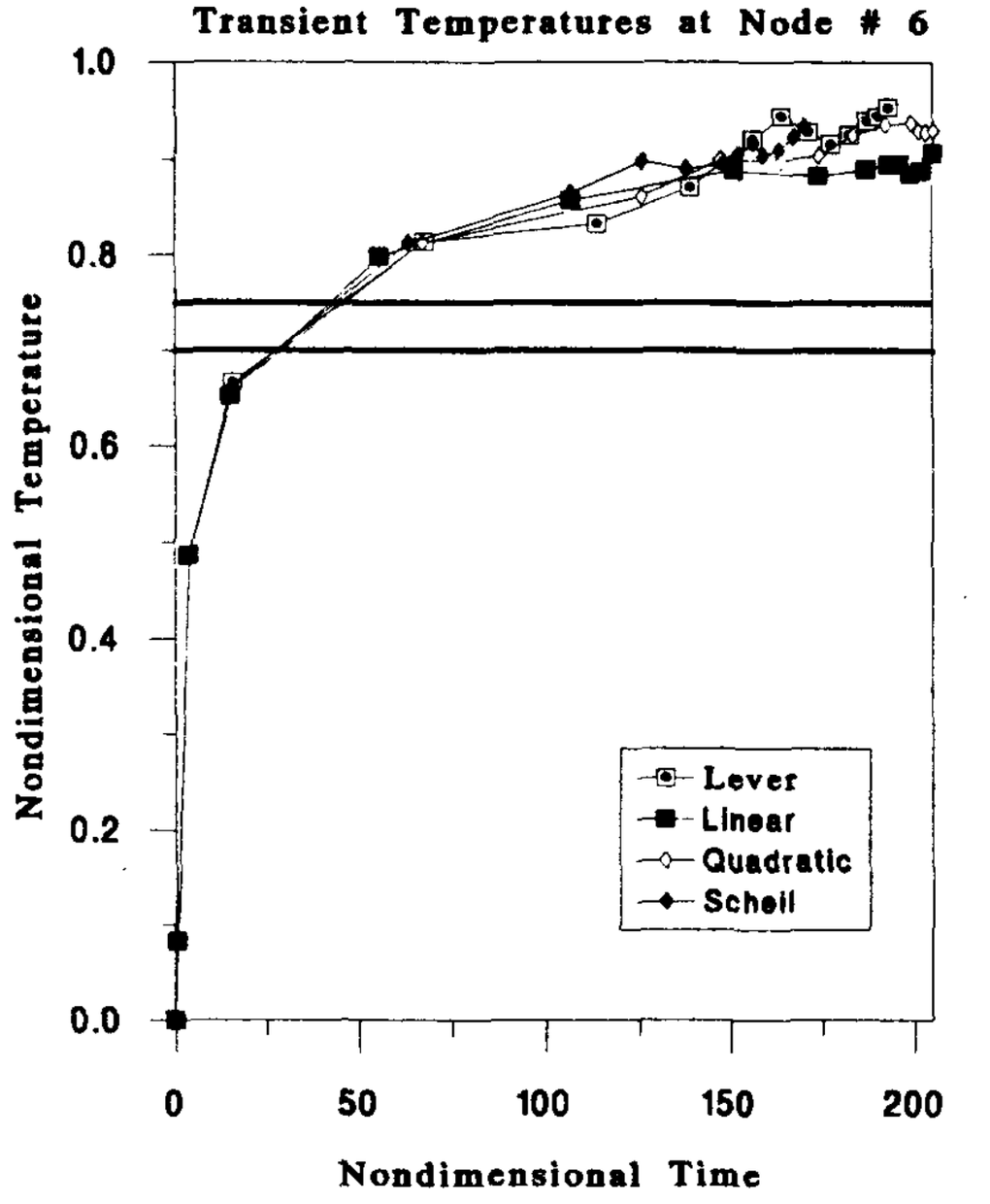

Figure 8. Temperature histories for a narrow mushy region at selected node points.

4. Conclusions

A numerical analysis of four latent heat models during the melting process was performed to evaluate the differences in each model. The specific heat method was used to

handle the phase-change phenomena at the interfaces. No explicit interface boundary conditions were required, so that the fixed grid scheme was employed in this analysis.

Four different latent heat models were employed to examine the melting pattern, the temperature history and the natural convection effect for two different mushy zones.

The numerical study shows a considerable disagreement between the models in the temperature history in the wide mushy zone. However, no significant difference was found in the narrow mushy zone. Therefore, a proper selection of latent heat model is essential to predict the exact temperature distribution during the phase-change process for alloys having wide mushy zones.

Nomenclatures

α: Thermal diffusivity
β: Volumetric thermal expansion coefficient
δ_{ij}: Kronecker delta
ρ: Density
μ: Viscosity
ν: Kinematic viscosity
c_p: Specific heat
f_s: Solid fraction
g: Gravity
k: Thermal conductivity
l: Reference distance
L: Latent heat
q_s: Source term
p: Pressure
P: Equilibrium partition
t: Time
T: Temperature
T_e: Eutectic temperature
T_m: Fusion temperature
T_{liq}: Temperature of liquidus
T_{sol}: Temperature of solidus
T_2: Maximum temperature
T_1: Minimum temperature
u: Velocity
U: Reference velocity

References

1. H.M. Ettouney and R.A Brown, "Finite Element Methods for Steady Solidification Programs", *J. of Comp. Phys.*, Vol. 49, pp. 118－124(1983)
2. N. Ramachandran, J.R. Gupta and Y. Jalunu, "Thermal and Fluid Flow Effects during the Solidification in a Cavity", *Int. J. Heat Mass Transfer,* Vol. 25, pp. 187－194(1982).
3. K. Morgan, "A Numerical Analysis of Freezing and Melting with Convection", *Comp. Meth. Appl. Engng.,* Vol. 28, pp. 275－284(1981).
4. V.R. Voller, N.C. Markatos and M. Cross, "An Enthalpy Method for Convection Diffusion Phase Changes", *Int. J. Num. Meth. Engng,* Vol. 24, 00. 271－284(1987).
5. V.R. Voller and C. Prakash, "A Fixed Grid Modeling Methodology for Convection Diffusion Mushy Region Phase-Change Problems", Int. J. Heat Mass Transfer, Vol. 30, pp. 1709－1719(1987).
6. C. Gau and R. Viskanta, "Melting and Solidification of a Metal System in a Rectangular Cavity", *Int. J. Heat Mass Transfer,* Vol. 27, pp. 113－123(1984).
7. J.H Kim ; *Simulation of Microsegregation during Binary Alloy Solidification,* Ph.D. Thesis, Georgia Institute of Technology(1990).
8. J.H. Kim and C.W. Meyers, "Studies of Solid-Liquid Interface Behaviors during Solidification Process", Accepted for Proc. *TMS Meeting,* San Diego(1992).
9. J.H. Kim and C.W. Meyers, "On Simulating Binary Alloy Solidification in Complex Geometries", Accepted for Proc. *TMS Meeting,* Hawaii(1992).
10. M.C. Flemings ; *Solidification Processing,* McGraw Hill(1974).
11. W. Kurz and D.J. Fisher ; *Fundamentals of Solidification,* 3rd ed. Trans Tech Publications(1989).
12. T.J. Chung ; *Finite Element Analysis in Fluid Dynamics,* McGraw Hill(1978).

13. J.H. Chen and H.L. Tsai, Comparison on Different Modes of Latent Heat Release for Modeling Casting Solidification, Cast Expo(April 1990).